Néel and valence-bond crystal order on a distorted kagome lattice: Implications for Zn-paratacamite

Erik S. Sørensen,[1,*] Michael J. Lawler,[2,3] and Yong Baek Kim[4]
[1]*Department of Physics and Astronomy, McMaster University, Hamilton, Ontario, Canada L8S 4M1*
[2]*Department of Physics, Applied Physics, and Astronomy, Binghamton University, P.O. Box 6000, Binghamton, New York 13902-6000, USA*
[3]*Department of Physics, Cornell University, Ithaca, New York 14853, USA*
[4]*Department of Physics, University of Toronto, Toronto, Ontario, Canada M5S 1A7*
(Received 19 February 2009; published 4 May 2009)

Zn-paratacamite is a rare spin-1/2 antiferromagnetic insulator with an ideal kagome lattice structure in part of its phase diagram. As a function of Zn doping, this material undergoes a structural distortion which relieves the frustration and introduces magnetic order in the ground state, though the precise nature of the order is not clear at this point. In this paper, we present strong evidence for Néel ordering in the *strongly* distorted phase of Zn-paratacamite through the application of quantum Monte Carlo techniques. These numerical results support a recent Schwinger-boson mean-field theory of Zn-paratacamite. For *weak* distortion, close to the ideal kagome limit, our results indicate a regime with no Néel order but with broken glide-plane symmetry. For this model the glide-plane symmetry is broken by *any* valence-bond crystal. Hence, our results lend support to recent proposals [P. Nikolic and T. Senthil, Phys. Rev. B **68**, 214415 (2003); R. R. P. Singh and D. A. Huse, Phys. Rev. B **76**, 180407(R) (2007)] of a valence-bond crystal ground state for the undistorted lattice. The phase transition between the two phases could be in the deconfined universality class if it is not a first-order transition.

DOI: 10.1103/PhysRevB.79.174403 PACS number(s): 75.10.Jm, 73.43.Nq, 75.40.Mg

I. INTRODUCTION

Recently, a number of spin-1/2 frustrated magnetic insulators have been discovered without any sign of magnetic order or structural distortions down to the lowest temperatures studied.[1–4] Among these materials, the Zn-doped-paratacamite family stands out for having a (nearly) controllable degree of distortion allowing the amount of geometric frustration to be tuned directly by an experimentalist. As such, they are a promising place to look for new phases of matter while at the same time probe how these new phases may be related to more well understood phases.

The control of the distortion is largely through the chemical pressure induced by the substitution of Zn atoms for Cu atoms on the (gray) triangular lattice planes that live in between kagome planes, as shown in Fig. 1. While Zn and Cu atoms are similar in size, Zn atoms fit into these sites without disrupting their environment, unlike Cu atoms which distort the kagome planes given a high enough density. In particular, for less than 0.3 filling of Zn atoms (greater than 0.7 filling of Cu atoms) the lattice distorts in a remarkable bipartite structure and magnetic order is found in the ground state.[3,5,6] The spins are thus relatively unfrustrated at these low doping concentrations. For Zn doping larger than this threshold, the lattice has the undistorted ideal kagome form and for $x \geq 0.4$ no magnetic ordering has been reported down to 50 mK despite an estimated spin exchange $J \sim 200$ K.[5]

A natural theoretical model of this material is the spin-1/2 Heisenberg model with two exchange parameters on a distorted kagome lattice[5–7] (see Fig. 1):

$$H = J \sum_{\langle i,j \rangle} \mathbf{S}_i \cdot \mathbf{S}_j + \lambda_D J \sum_{\langle\langle ij \rangle\rangle} \mathbf{S}_i \cdot \mathbf{S}_j. \quad (1)$$

Here λ_D tunes the distortion on the next-nearest-neighbor bonds (nnn) with $\lambda_d = 1$ the undistorted ideal kagome limit (where nnn bonds are equivalent to nn bonds). This is an idealized model for several reasons: it assumes the coupling between planes and further neighbors is weak (which seems reasonable[5,6]), it neglects Dzyaloshinsky-Moria interactions possibly important for the low-temperature susceptibility,[8,9]

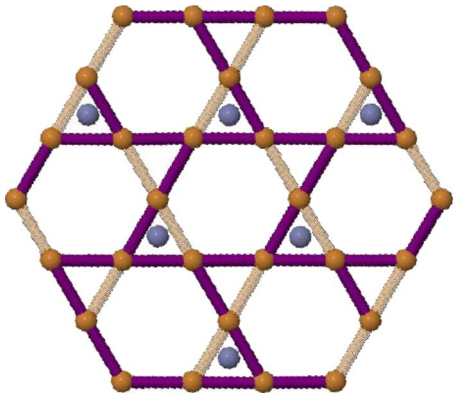

FIG. 1. (Color online) The layered Zn-paratacamite magnetic lattice structure. Cu atoms live on the (sometimes distorted) kagome layer (bronze atoms) while Zn or Cu atoms occupy sites on a triangular lattice above the kagome plane (gray atoms). Solid (purple) bonds represent nearest neighbors [$\langle ij \rangle$ in Eq. (1)] resulting in a "brick-wall" lattice, while transparent (bronze) bonds represent the next-nearest neighbors [$\langle\langle ij \rangle\rangle$ in Eq. (1)].

and it replaces the effect of doping in the triangle lattice planes with the uniform distortion parameter λ_D. While it is possible that any of these approximations may be important for some properties of Zn-paratacamite, here we will focus on those properties which clearly belong to the phenomenology of this simplified model.

In this paper, we study the ground-state properties of the Hamiltonian in Eq. (1) as a function of λ_D, extrapolating between a bipartite "brick-wall" lattice at $\lambda_D=0$ and the isotropic kagome lattice at $\lambda_D=1$. At $\lambda_D=0$, we show using valence-bond quantum Monte Carlo[10,11] that the ground state is magnetically ordered with the expected Néel pattern for this bipartite lattice and with a magnetization of $m^\dagger=0.240(1)$ that is 22% smaller than the square lattice value.[12] For $0\leq\lambda_D\leq 1$ we study this model using exact diagonalization on finite-size clusters of size 12, 24, and 36 sites. By introducing symmetry breaking fields, we study the susceptibility of the ground state toward dimerization. Remarkably, we find that for $\lambda_D\gtrsim 0.8$, a phase transition occurs toward a rotationally invariant state which prefers to have a broken glide-plane (GP) symmetry, consistent with the presence of a valence-bond crystal (VBC) order including the pin-wheel VBC pattern proposed by Ref. 7. This symmetry breaking survives up to the $\lambda_D=1$ ideal kagome limit. While it is difficult to draw definitive conclusions on such small systems, a broken glide-plane symmetry supports Refs. 13–15 proposal that the spin-1/2 kagome antiferromagnet has a VBC ground state. At the same time a broken glide-plane symmetry is not consistent with a spin-liquid phase, frequently supported by other exact diagonalization studies.[16] In addition, while we cannot rule out a first-order transition from a VBC phase to the Néel phase in our model, it is also possible this quantum phase transition is in the deconfined universality class.[17]

II. RESULTS AT $\lambda_D=0$

We first discuss our results obtained at $\lambda_D=0$ where we have been able to study large system. As can be seen from Fig. 1, where the transparent (bronze) bonds are proportional to λ_D, the lattice formed by the remaining solid (purple) bonds is a bipartite "brick-wall" lattice with a coordination number of 3 on two thirds of the sites and of 2 on the remaining sites. Due to the bipartite nature of the $\lambda_D=0$ lattice there is no frustration. A classical antiferromagnetic Néel state can be unambiguously assigned to the lattice. It is then possible to perform very efficient quantum Monte Carlo simulations using the recently proposed[10,11] valence-bond quantum Monte Carlo (VBQMC). For $\lambda_D=0$ there is no sign problem and extremely precise results can be obtained. VBQMC is a projection method where the $T=0$ ground state is projected out through the repeated application of the Hamiltonian, H, on a trial state, $|\Psi_T\rangle$. In essence, $|\Psi_G\rangle=(-H)^n|\Psi_T\rangle$. In the limit where $n\to\infty$ this becomes exact. In a practical implementation n is kept fixed at a high number and the different terms in $|\Psi_G\rangle$ are sampled using Monte Carlo methods. For convergence, the relevant lattice size-independent expansion order is n/N_b, where N_b is the number of terms in the Hamiltonian. N_b is equal to $(4/3)N$ for the brick-wall lattice, with N as the number of sites in the lattice. Typically we use $n/N_b=3-10$ and an extrapolation to $n/N_b=\infty$ can then be performed.

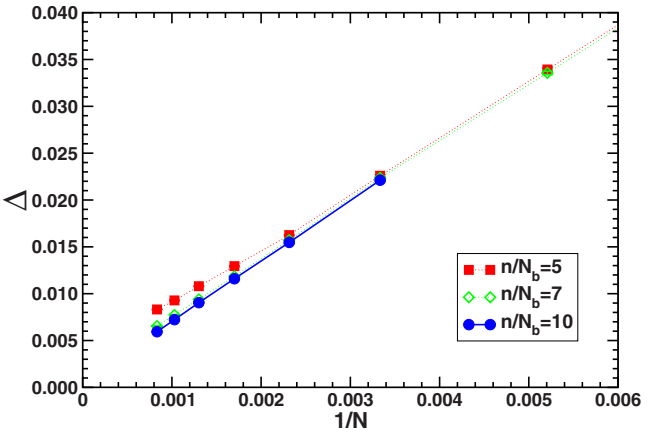

FIG. 2. (Color online) The singlet-triplet gap, Δ, versus inverse system size $1/N$. The different curves correspond to different expansion orders n, with the ratio n/N_b kept fixed. Here, N_b is the number of bond operators in the Hamiltonian, $N_b=(4/3)N$. Results are shown for $n/N_b=5$ (■), $n/N_b=7$ (◇), and $n/N_b=10$ (●). Error bars are shown but are typically smaller than the symbols.

We have performed systematic VBQMC studies of $\lambda_D=0$ brick-wall lattices with number of sites $N=12\times m^2$ for $m=1,\ldots,10$ using periodic boundary conditions. Typically, 10^6-10^7 Monte Carlo steps were performed for a range of values of $n/N_b=3,5,7,10$. All error bars were calculated using standard binning techniques.

A very natural question to ask is if the $\lambda_D=0$ brick-wall lattice has a nonzero singlet to triplet gap, Δ. A particularly appealing feature of VBQMC is that it allows for a direct estimator[10,11] of this gap independent of the estimators for the ground-state singlet and excited triplet energies. Due to a cancellation of errors it is then possible to calculate this gap with a precision significantly exceeding that which could have been obtained by separately calculating the ground and excited state energies. Our results for Δ at $\lambda_D=0$ are shown in Fig. 2. Data are shown for three different values of $n/N_b=5$ (■), $n/N_b=7$ (◇), $n/N_b=10$ (●) versus inverse system size $1/N$. At $N=1200$, $n/N_b=10$ the gap is $\Delta=0.0059(1)J$ and minimal dependence on the expansion order n/N_B is seen. From the results shown in Fig. 2 we conclude that the gap vanishes in the thermodynamic limit.

For the two-dimensional square lattice antiferromagnetic Heisenberg model it is well known[18] that the antiferromagnetic order exists at $T=0$ with $m^\dagger=0.30743(1)$ (Ref. 12). The square lattice has a coordination number of 4 whereas the brick-wall lattice has a mixed coordination of 2 and 3. We therefore expect $m^\dagger$ to be smaller or possibly zero for the brick-wall lattice. As usual, we define

$$S(\mathbf{q}_c)=\frac{1}{N^2}\left\langle\left(\sum_{x,y}\tilde{S}^z(x,y)\right)^2\right\rangle, \tag{2}$$

where $\mathbf{q}_c$ is the wave vector of the staggered magnetization and $\tilde{S}^z(x,y)$ is given by

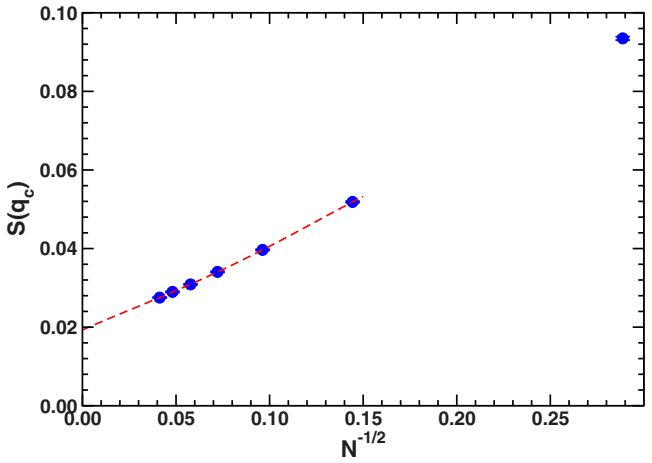

FIG. 3. (Color online) The structure factor, $S(\mathbf{q}_c)$, versus inverse linear system size $1/\sqrt{N}$. Results are shown for $n/N_b=10$. Error bars are shown but are typically smaller than the symbols. Results for $n/N_b=7$ are indistinguishable from the $n/N_b=10$ results shown and have been left out for clarity.

$$\tilde{S}^z(x,y) = \frac{1}{2}\epsilon_{x,y}\sigma^z(x,y), \tag{3}$$

with $\epsilon_{x,y}$ equal to +1 or −1 depending on what sublattice the point (x,y) belongs to. Hence we have[18]

$$m^\dagger = \langle \tilde{S}_i^z \rangle = \lim_{L\to\infty} \sqrt{3S(\mathbf{q}_c)}. \tag{4}$$

Our results for $S(\mathbf{q}_c)$ for $n/N_b=10$ are shown in Fig. 3. It is expected[18] that the leading finite-size corrections are of the form $1/\sqrt{N}$ and a fit to this form yields $S(\mathbf{q}_c)=0.0192(5)$ and consequently

$$m^\dagger = 0.240(3). \tag{5}$$

As expected, this value is reduced with respect to the square lattice result, but is clearly nonzero, indicating a well-established antiferromagnetic order at $\lambda_D=0$.

III. RESULTS AT $\lambda_D \neq 0$

We now turn to a discussion of our results for $0<\lambda_D \leq 1$. In this case it is no longer possible to perform VBQMC calculations due to a sign problem that appears rather severe as soon as $\lambda_D \neq 0$ and reliable numerical results are therefore much harder to obtain. In light of the strong sign problem we have performed exact diagonalization studies for $0<\lambda \leq 1$ on finite-size systems employing periodic boundary conditions. Our goal is to study generalized bond susceptibilities with respect to symmetry breaking fields. We focus on C_2 and GP symmetry breaking fields shown in Fig. 4 where the dimers indicate bonds where the strength is modified $J'=J\pm\delta$. The C_2 symmetry corresponds to a rotation by π and clearly the field shown in Fig. 4(a) breaks this symmetry. The GP symmetry[7] is somewhat more exotic and corresponds to a translation along the rails where the dimers are sitting followed by a reflection around one of these rails. We note that the GP field does not break the C_2 symmetry and likewise the

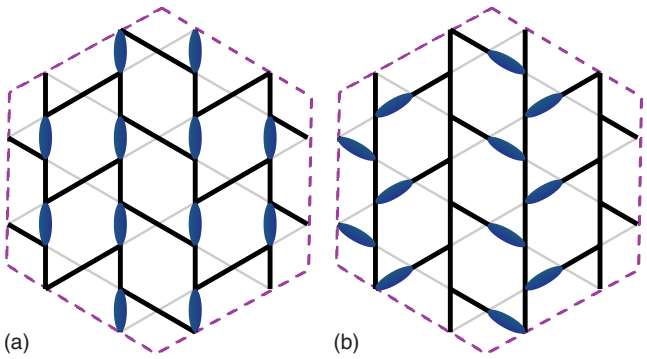

FIG. 4. (Color online) (a) The glide-plane symmetry breaking field. (b) C_2 symmetry breaking field. Solid dimers denote bonds where the coupling strength is modified to J'.

C_2 field preserves the GP symmetry. The pin-wheel VBC discussed in Ref. 7 would break the GP symmetry but not the C_2 symmetry where as the columnar VBC (Ref. 7) would break both. If we by $\mathbf{b}, \mathbf{b}_{C_2,\mathrm{GP}}$ denote the ground-state expectation value $\langle \mathbf{S}_i \cdot \mathbf{S}_j \rangle$ for the bond $\mathbf{b}$ and its partner under the symmetry operation $\mathbf{b}_{C_2,\mathrm{GP}}$, we can define the generalized bond susceptibility as follows:

$$\chi_{C_2,\mathrm{GP}} = \lim_{\delta\to 0} \frac{|\Delta\mathbf{b}_{C_2,\mathrm{GP}}(J'=J+\delta) - \Delta\mathbf{b}_{C_2,\mathrm{GP}}(J'=J-\delta)|}{2\delta}, \tag{6}$$

with

$$\Delta\mathbf{b}_{C_2,\mathrm{GP}} = \mathbf{b}(J') - \mathbf{b}_{C_2,\mathrm{GP}}(J). \tag{7}$$

Clearly, if $\Delta\mathbf{b}$ goes to zero linearly with δ the generalized bond susceptibility is a constant independent of system size and the associated symmetry is not spontaneously broken. On the other hand, a bond susceptibility diverging with system size signals that the associated symmetry is spontaneously broken in the thermodynamic limit.

When performing exact diagonalization studies of small systems the choice of the finite cluster is crucial since the smaller clusters will reduce the point group symmetry of the infinite lattice. For the isotropic kagome lattice, $\lambda_D=1$, the plane group is *p6mm*. This symmetry group implies that for the isotropic kagome lattice all bonds are equivalent. Our choice of finite clusters are shown in Fig. 5 for $N=12,24,36$. Only the $N=36$ cluster has the full symmetry point group symmetry of the kagome lattice. However, for all clusters do we find that all bonds are equivalent at $\lambda_D=1$. For $0<\lambda_D<1$ only two different types of bonds occur for these clusters. These are the only clusters we have found with these properties. For the bond susceptibilities to yield meaningful information about the thermodynamic limit this is very important since we want to make sure that the presence of a reduced point group symmetry does not explicitly break the C_2 or GP symmetry. This is not the case for the clusters shown in Fig. 5.

Using the clusters from Fig. 5 we can now study χ_{GP} and χ_{C_2} as a function of λ_D for the different clusters. Our results are shown in Figs. 6 and 7, respectively. We have used δ

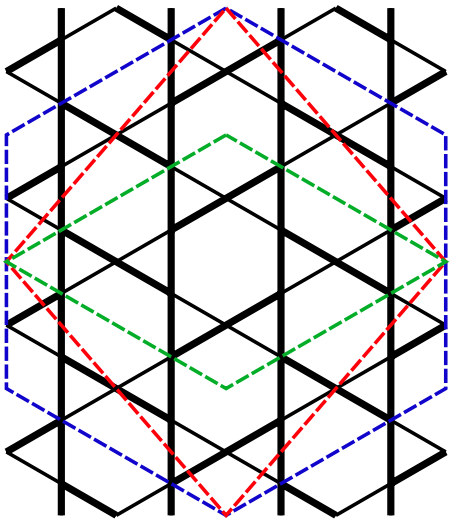

FIG. 5. (Color online) The 12-, 24-, and 36-site lattices.

≤ 0.001 small enough that χ, Eq. (6), is almost completely independent of δ. We begin by discussing χ_{GP} shown in Fig. 6. For λ_D less than roughly ~ 0.8 do we find that χ_{GP} is almost independent of N. In the inset is shown $1/\chi_{\mathrm{GP}}$ as a function of $1/N$ for $\lambda=0.3$ indicating a finite value in the thermodynamic limit. This is consistent with the GP symmetry not being broken. However, for λ_D greater than ~ 0.8 pronounced size dependence occurs. At $\lambda_D=1$, $1/\chi_{\mathrm{GP}}$ as a function of $1/N$ is shown in the inset. In this case it seems reasonable to conclude that χ_{GP} diverges with N and hence that the GP symmetry is spontaneously broken in the thermodynamic limit. A natural interpretation of this result is that a quantum phase transition occurs at ~ 0.8 between a state with antiferromagnetic order, which does not break the GP symmetry, to a *new* phase where the GP symmetry is *broken*.

Finally, in Fig. 7 we show our results for χ_{C_2}. Again we see that for λ_D smaller than roughly ~ 0.8 there is very little N dependence. In the inset of Fig. 7 is shown $1/\chi_{C_2}$ as a function of $1/N$ at $\lambda_D=0.3$. Clearly the results extrapolate to

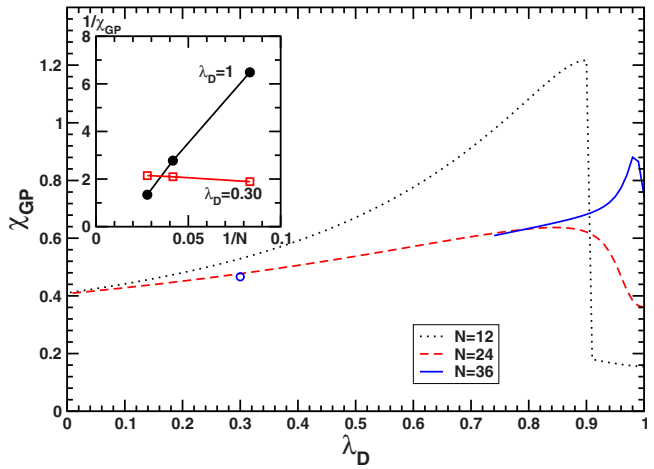

FIG. 6. (Color online) The glide-plane susceptibility, χ_{GP} as a function of λ_D for the different system sizes, $N=12,24,36$. The circles represent results for $N=36$, $\lambda_D=0.3$. The inset shows χ_{GP}^{-1} versus $1/N$ at $\lambda_D=0.3,1.0$.

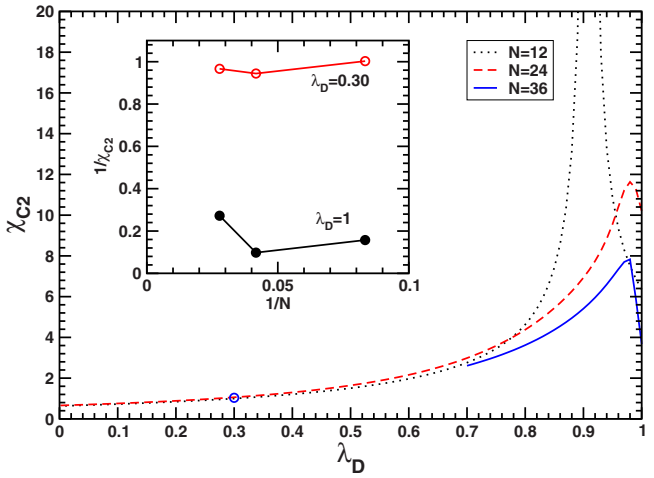

FIG. 7. (Color online) The C_2 susceptibility χ_{C2} as a function of λ_D for the different system sizes, $N=12,24,36$. The circles represent results for $N=36$, $\lambda_D=0.3$. The inset shows χ_{C2} versus $1/N$ at $\lambda_D=0.3,1.0$.

a finite value in the thermodynamic limit consistent with the absence of C_2 symmetry breaking as would be the case for an antiferromagnetic phase. As before, we find that for λ_D greater than roughly ~ 0.8 pronounced finite-size effects occur consistent with a quantum phase transition. However, in this case, as can be seen in the inset of Fig. 7 at $\lambda_D=1$, the susceptibility *does not diverge* but rather tends to a finite, possibly very small value in the thermodynamic limit. Therefore, in the new phase occurring for λ_D greater than 0.8 the C_2 symmetry is not broken.

It is important to realize that several finite cluster effects are present in Figs. 6 and 7. First, the abrupt change in χ_{GP} for $N=12$ in Fig. 6 is due to a level crossing that does not occur for $N=24,36$. The presence of such level crossings for small clusters is not surprising. Second, even though we believe that we can reliably detect the divergence of χ_{GP}, the eventual ordering occurring for $\lambda_D>0.8$ may not be compatible with the $N=12,24$ clusters. For example, the $N=12,24$ sized systems do not possess the translational symmetry of the large unit cell expected for the MZ state of Fig. 8(a). This could explain the relatively different appearance of the results for $N=24,36$ in Fig. 6.

IV. DISCUSSION

Given these results, we may draw several conclusions. At $\lambda_D=0$, we have demonstrated that the spin gap vanishes and that the ground state has a finite staggered magnetization that is 22% smaller than the square lattice value. We find this surprising given that each site has either two or three neighbors (with 2.67 neighbors on average) and that this network is not far from the one-dimensional chain model which is disordered. It appears that this form of dimensional reduction does not easily suppress magnetic order.

While we could only study very small system sizes for $\lambda_D>0$, finite-size effects seem to be small all the way out to $\lambda_D\approx 0.8$. As a result, the antiferromagnetic order is quite

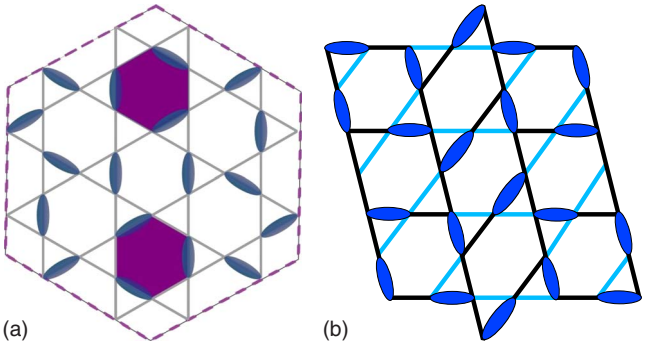

FIG. 8. (Color online) (a) The Marston and Zeng (MZ) dimer pattern (Ref. 19) on the kagome lattice and (b) the pin-wheel state on the distorted kagome lattice (Ref. 7). The MZ pattern arises by maximizing the number of dimers around each hexagon. Notice how the dimers on the two highlighted hexagons can be rotated by 180 about the center of the hexagon without needing to alter the rest of the dimer pattern. This benzenelike resonance suggests that rotational symmetry may be only very weakly broken if this is the ground state. The pin-wheel pattern, on the other hand, maximizes dimers around each rhombus and is manifestly C_2 rotationally symmetric about each hexagon.

robust and appears to be the ground state with a large basin of stability.

The ground state for $0.8 \lesssim \lambda_D \leq 1$ appears to break the glide-plane symmetry while remaining invariant under C_2 rotations. While larger systems would be required to make definitive conclusions, this evidence is in stark contrast to the prediction that the kagome lattice ground state is a spin liquid.[19,20]

Remarkably, on this lattice all valence-bond crystals break the glide-plane symmetry (the most glide-plane symmetric configuration of Fig. 4(b) still breaks glide-plane symmetry if the missing dimers are added to the picture). So the breaking of glide-plane symmetry strongly supports recent proposals[13–15] that the ground state may be a VBC. Candidate such states include the Marston and Zeng 36-site unit cell dimer (spin singlet) pattern (MZ)[19] and the pin-wheel pattern (in the presence of distortion) (see Fig. 8). One may argue that the MZ pattern should also break C_2 rotational symmetry. However, such a symmetry may naturally be restored by benzenelike resonances on the three dimer hexagons. One should note that whether the recent ED results[16] are disfavoring the MZ VBC state as well as other proposed VBC states[13,21] or not, is a subject of intense debate.[15]

Since any VBC will have a diverging glide-plane susceptibility the results presented here are not very sensitive to transitions between different VBC's as long as they conserve C_2 symmetry. For example, a transition from the MZ pattern at $\lambda_D=1$ to the pin-wheel pattern at $\lambda_D<1$ is certainly possible. For $0.8 \lesssim \lambda_D$ we can therefore not exclude the presence of several different C_2 symmetric VBC phases although the rate of divergence of χ_{GP} could potentially be quite different for different phases. In fact, one might speculate that the cusp in χ_{GP} for $N=36$ and in χ_{C2} for $N=24,36$ in both cases at $\lambda_D^c=0.98$ is a signature of a phase transition between different valence-bond crystals.

A phase transition near $\lambda_D \approx 0.8$ was also found in the large-N study of Ref. 7. Thus both large-N and exact diagonalization methods predict the existence of a quantum phase transition at a value of λ_D away from the ideal kagome limit. If we assume that the spin gap is nonzero at $\lambda_D=1$ and vanish approximately linearly with the deviation of λ_D from 1, then this value for the quantum critical point is also roughly consistent with the vanishing of the spin gap (which, from exact diagonalizations, is estimated to be rather small but finite[20,22] in the thermodynamic limit and has a value of $0.1848J$ at $\lambda_D=1$ for the 36-site cluster). Given the apparent glide-plane symmetry breaking for $\lambda_D \gtrsim 0.8$, this phase transition then appears to be between two phases with *unrelated orders*. It may therefore fall into the deconfined universality class[17] if it is not a first-order transition.

ACKNOWLEDGMENTS

We thank Young Lee and Seung-Hun Lee for useful discussions. This work was supported by the Natural Sciences and Engineering Research Council of Canada (E.S.S. and Y.B.K.), the Canadian Foundation for Innovation (E.S.S.), the Canadian Institute for Advanced Research and the Canada Research Chair Program (Y.B.K.). E.S.S. gratefully acknowledges the hospitality of the Department of Physics at the University of Toronto where part of this work was carried out. This work was made possible by the facilities of the Shared Hierarchical Academic Research Computing Network (SHARCNET:www.sharcnet.ca).

*sorensen@mcmaster.ca

[1] Y. Shimizu, K. Miyagawa, K. Kanoda, M. Maesato, and G. Saito, Phys. Rev. Lett. **91**, 107001 (2003).
[2] Z. Hiroi, M. Hanawa, N. Kobayashi, M. Nohara, and H. Takagi, J. Phys. Soc. Jpn. **70**, 3377 (2001).
[3] J. S. Helton, K. Matan, M. P. Shores, E. A. Nytko, B. M. Bartlett, Y. Yoshida, Y. Takano, A. Suslov, Y. Qiu, J.-H. Chung, D. G. Nocera, and Y. S. Lee, Phys. Rev. Lett. **98**, 107204 (2007).
[4] Y. Okamoto, M. Nohara, H. Aruga-Katori, and H. Takagi, Phys. Rev. Lett. **99**, 137207 (2007).
[5] S.-H. Lee, H. Kikuchi, Y. Qiu, B. Lake, Q. Huang, K. Habicht, and K. Kiefer, Nature Mater. **6**, 853 (2007).
[6] J.-H. Kim, S. Ji, S.-H. Lee, B. Lake, T. Yildirim, H. Nojiri, H. Kikuchi, K. Habicht, Y. Qiu, and K. Kiefer, Phys. Rev. Lett. **101**, 107201 (2008).
[7] M. J. Lawler, L. Fritz, Y. B. Kim, and S. Sachdev, Phys. Rev. Lett. **100**, 187201 (2008).
[8] M. Rigol and R. R. P. Singh, Phys. Rev. Lett. **98**, 207204 (2007).
[9] M. Tovar, K. S. Raman, and K. Shtengel, Phys. Rev. B **79**, 024405 (2009).
[10] K. Beach and A. W. Sandvik, Nucl. Phys. B **750**, 142 (2006); http://www.sciencedirect.com/science/article/B6TVC-

4K7FFKT-1/2/c97ff1735c126caf67146012a075e6cd
[11] A. W. Sandvik, Phys. Rev. Lett. **95**, 207203 (2005).
[12] A. W. Sandvik and H. G. Evertz, arXiv:0807.0682 (unpublished).
[13] P. Nikolic and T. Senthil, Phys. Rev. B **68**, 214415 (2003).
[14] R. R. P. Singh and D. A. Huse, Phys. Rev. B **76**, 180407(R) (2007).
[15] R. R. P. Singh and D. A. Huse, Phys. Rev. B **77**, 144415 (2008).
[16] G. Misguich and P. Sindzingre, J. Phys.: Condens. Matter **19**, 145202 (2007).
[17] T. Senthil, A. Vishwanath, L. Balents, S. Sachdev, and M. P. A. Fisher, Science **303**, 1490 (2004).
[18] J. D. Reger and A. P. Young, Phys. Rev. B **37**, 5978 (1988).
[19] J. B. Marston and C. Zeng, 35th Annual Conference on Magnetism and Magnetic Materials; J. Appl. Phys. **69**, 5962 (1991).
[20] C. Waldtmann, H.-U. Everts, B. Bernu, C. Lhuillier, P. Sindzingre, P. Lecheminant, and L. Pierre, Eur. Phys. J. B **2**, 501 (1998).
[21] A. V. Syromyatnikov and S. V. Maleyev, Phys. Rev. B **66**, 132408 (2002).
[22] P. Lecheminant, B. Bernu, C. Lhuillier, L. Pierre, and P. Sindzingre, Phys. Rev. B **56**, 2521 (1997).